Portland State University

PDXScholar

Physics Faculty Publications and Presentations

Physics

2-1996

Adsorption of ruthenium red to phospholipid membranes

Pavel Smejtek
Portland State University

D. Voelker

Let us know how access to this document benefits you.

Follow this and additional works at: http://pdxscholar.library.pdx.edu/phy_fac

Part of the Biophysics Commons

Citation Details

Adsorption of Ruthenium Red to Phospholipid Membranes

Dirk Voelker and Pavel Smejtek

Department of Physics, Environmental Sciences and Resources Doctoral Program, Portland State University, Portland, Oregon 97207 USA

ABSTRACT   We have measured the distribution of the hexavalent ruthenium red cation (RuR) between water and phospholipid membranes, have shown the critical importance of membrane negative surface charge for RuR binding, and determined the association constant of RuR for different phospholipid bilayers. The studies were performed with liposomes made of mixtures of zwitterionic L-α-phosphatidylcholine (PC), and one of the negatively charged phospholipids: L-α-phosphatidylserine (PS), L-α-phosphatidylinositol (PI), or L-α-phosphatidylglycerol (PG). Lipid composition of PC:PX membranes was 1:0, 19:1, 9:1, and 4:1. Liposomes were processed using freeze-and-thaw treatment, and their size distribution was characterized by light scattering and electron microscopy. Experimental distribution isotherms of RuR obtained by ultracentrifugation and spectrophotometry can be reproduced with the Langmuir-Stern-Grahame model, assuming that RuR behaves in the diffuse double layer as an ion with effective valency <6. In terms of this model, PC-PS, PC-PI, and PC-PG membranes were found to be electrostatically equivalent and the intrinsic association constants of RuR were obtained. RuR has highest affinity to PS-containing membranes; its association constant for PC-PI and PC-PG membranes is about 5 times smaller than that for PC-PS membranes. From the comparison of RuR binding to mixed negatively charged phospholipid membranes and RuR binding to sarcoplasmic reticulum (SR), we conclude that the low-affinity RuR binding sites may indeed be associated with the lipid bilayer of SR.

INTRODUCTION

Ruthenium red (RuR) was discovered in 1892 (Joly, 1892). It is an inorganic, intensely colored compound prepared from $RuCl_3$ in a NH_3 solution and never occurs in nature. Mangin first described the staining properties of RuR to visualize pectin in plant cells (Mangin, 1893), and since then it has been widely used in biology. RuR is used in light microscopy as a generic stain for polyanions with a high charge density (Murano et al., 1990). Reimann published the first electron micrographs employing RuR as a stain (Reimann, 1961), and several authors extensively discussed its usage for electron microscopy (Dierichs, 1979; Luft, 1971a,b).

In addition to its staining properties, RuR is an extremely potent modulator of biological activity. The spectrum of RuR activity is broad because RuR associates with numerous Ca^{2+}-binding proteins (Charuk et al., 1990). Because of its association with Ca^{2+}-binding proteins, RuR interferes with the function of the Ca^{2+} ion as a chemical messenger. For example, RuR is a potent inhibitor of Ca^{2+} uptake and Ca^{2+} release in mitochondria (Moore, 1971; Vasington et al., 1972; Luthra and Olson, 1977). RuR is known to inhibit Ca^{2+} pump activity in membranes (Watson et al., 1971) and to block the release of Ca^{2+} from the sarcoplasmic reticulum (Salama and Abramson, 1984). RuR interference with

nerve transmission is related to the reduction of neurotransmitter release (Taipale et al., 1989). Another example is the RuR-induced alteration of the enzymatic activity of the Ca^{2+}-binding protein calmodulin (Sasaki et al., 1992). The use of RuR in sensory neuron research has been reviewed by Amann and Maggi (1991). Because of the well-documented action of RuR on Ca^{2+}-dependent events, it has been extensively used in studies of Ca^{2+} binding sites in proteins. Most studies of the effects of RuR in biomembranes have been focused on proteins, but little is known about the interaction of RuR with the lipid matrix of biomembranes. The objective of this work was to study the binding of RuR to well-defined phospholipid bilayer membranes.

In an aqueous environment RuR is present as a hexavalent cation (Carrondo et al., 1980; Fletcher et al., 1961)

$$[(NH_3)_5Ru^{III} - O - (NH_3)_4Ru^{IV} - O - Ru^{III}(NH_3)_5]^{+6},$$
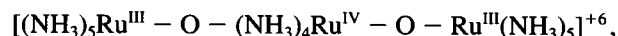
which, due to its high positive charge, is expected to be very responsive to negative charges on proteins, lipid membranes, and cation carriers. The significance of electrostatic effects in RuR binding follows from the expectation that the distribution of the hexavalent RuR cation in the vicinity of negatively charged groups on biomembranes will be determined approximately by a Boltzmann factor, $\exp(-6eV/kT)$, where V is the local electrostatic potential.

The possibility of electrostatically mediated action of RuR in biomembranes in relation to its adsorption to negatively charged lipids has been already considered in the literature. Moutin et al. (1992) proposed that the low-affinity Ca^{2+} binding sites in SR membranes may originate from lipids in the vicinity of Ca^{2+}-ATPase. Another case of electrostatically mediated action of RuR was invoked in the

mechanism of inhibition of the Ca^{2+} pump in the plasma membrane and in the rationalization of the stimulating effect of negatively charged lipids. It was proposed that the inhibition of the Ca^{2+} pump by RuR is of electrostatic origin, mediated by the neutralization of negatively charged phospholipids by adsorbed RuR cations (Missiaen et al., 1990). Adsorption of ions to lipid membranes has recently been reviewed by Tatulian (1993).

In view of the extensive use of RuR in studies of biological membranes and the lack of quantitative data on adsorption of RuR to lipid bilayers, we have measured the distribution of RuR between water and liposomes with a well-defined surface charge density. The study was done with liposomes prepared from mixtures of zwitterionic phosphatidylcholine (PC) and one of the negatively charged lipids: phosphatidylserine (PS), phosphatidylinositol (PI), or phosphatidylglycerol (PG). RuR was found to have higher affinity to PS-containing membranes relative to PC-PG and PC-PI membranes. We show that the distribution isotherms can be reproduced with the Langmuir-Stern-Grahame adsorption model (also called the Gouy-Chapman-Stern model with mass action formalism or mass action equations). Within the framework of this model the hexavalent RuR behaves as a cation with effective valency <6. In addition, effective valency was found to be a function of the membrane surface charge density. We also discuss adsorption of RuR to lipid matrix of biomembranes. Using the sarcoplasmic reticulum (SR) membrane as a prototype biomembrane and the binding parameters of RuR for negatively charged phospholipids obtained in this work, we conclude that adsorption of RuR to the lipid matrix of SR can account for RuR adsorption to the so-called low-affinity binding sites of SR.

THEORY

Adsorption of RuR to the lipid bilayer is determined from the decrease of RuR concentration caused by the adsorption of RuR to liposome membranes. The distribution of RuR between the liposome membranes and the aqueous phases is measured according to

$$R_{RuR} = \frac{[RuR]_{eq}}{[RuR]_{init}}, \qquad (1)$$

where $[RuR]_{eq}$ is the aqueous concentration of RuR in the presence and $[RuR]_{init}$ is the RuR concentration in the absence of liposomes. The ratio R_{RuR} varies between 0 and 1; the smaller the R_{RuR}, the greater the adsorption. The dependence of R_{RuR} on $[RuR]_{init}$ is defined as the distribution isotherm.

The equilibrium concentration $[RuR]_{eq}$ depends on the adsorption of RuR to the bilayer, namely on the membrane surface density of RuR, $(RuR)_m$. For bilayers prepared from the two types of phospholipids, electrically neutral PC and negatively charged PX (PX represents one of the charged

lipids PS, PI, or PG), the balance of free and bound RuR ions is given by

$$[RuR]_{eq} + (RuR)_m(P_{PX}[PX] + P_{PC}[PC]) = [RuR]_{init}. \qquad (2)$$

P_{PX} and P_{PC} designate the area per lipid of negatively charged and neutral lipids, and [PX] and [PC] are their respective concentrations in the suspension of liposomes. A similar balance equation is needed, in principle, for the monovalent cations. In modeling RuR adsorption it was assumed that the concentration of monovalent cations in water did not appreciably change, $[CAT]_{eq} \approx [CAT]_{init}$ (this simplification is justifiable in view of the rather small binding constant of potassium ions to negatively charged lipids ($1\ M^{-1}$) and the experimental conditions).

Experimental data were analyzed in terms of two versions of a model originally proposed by McLaughlin and Harary (1976), which combines Langmuir adsorption isotherms with the Gouy-Chapman theory of the diffuse double layer. This model has been found adequate for a number of adsorbing species (McLaughlin, 1989).

Two models of RuR adsorption, designated A and B, are considered. In model A the adsorption sites are only the negatively charged lipids; in model B adsorption to membrane lipids is assumed to be nonselective. Both models include co-adsorption of RuR and monovalent ions (CAT) to phospholipid bilayers, which is described by a Langmuir adsorption isotherm. Accordingly, the membrane surface density of RuR ions, $(RuR)_m$, depends upon the association constant, K_{mRuR}, the concentration of RuR adjacent to the membrane surface (in view of the fact that some liposomes may be multilamellar, it is assumed that RuR does not form "trans" complexes between lamellae), $[RuR]_{if}$, and the density of sites available to RuR cations, f_{RuR}. Similar equation holds for monovalent cations, such as potassium, therefore

$$(RuR)_m = K_{mRuR}[RuR]_{if}f_{RuR} \qquad (CAT)_m$$

$$(3)$$

$$= K_{mCAT}[CAT]_{if}f_{CAT}.$$

A Boltzmann relation is used to relate the interfacial concentrations of adsorbing species to their concentrations in the bulk solution

$$\frac{[RuR]_{if}}{[RuR]_{eq}} = \exp\left(-\frac{z_{RuR,eff}eV_m}{k_BT}\right) \quad \frac{[CAT]_{if}}{[CAT]_{eq}} = \exp\left(-\frac{eV_m}{k_BT}\right). \qquad (4)$$

V_m is the electrostatic potential at the membrane surface. To fit the experimental results, it became necessary to introduce an effective charge of the hexavalent cation RuR, $z_{RuR,eff}e$.

The membrane surface charge density σ_m depends on the charge density of the native PC-PX membrane, σ_0, and on the surface densities of adsorbed cations,

$$\sigma_m = \sigma_0 + e(CAT)_m + 6e(RuR)_m. \qquad (5)$$

Factor "6" associated with the surface density of adsorbed RuR reflects the fact that physical charge of RuR is +6

(experimental results are consistent with this assumption and suggest "anomalous" behavior of RuR within the diffuse double layer). Grahame's equation relates σ_m to V_m,

$$\sigma_m = \left\{ (2\epsilon_w\epsilon_0 k_B T) \sum C_i \left[\exp\left(\frac{-z_i e V_m}{k_B T} \right) - 1 \right] \right\}^{1/2}, \quad (6)$$

where C_i is the bulk concentration of ions of valency z_i in the suspension, including RuR and counter-ions.

Model A

In Model A RuR and monovalent salt cations bind exclusively to negatively charged lipids in the bilayer, forming 1:1 complexes. Thus adsorption is lipid specific, and both ions compete for the free, unoccupied, negatively charged lipids.

$$(RuR)_m + (CAT)_m + f = Q_{PX}, \quad (7)$$

where f is the membrane surface density of unoccupied negatively charged lipids. In model A the adsorption sites for RuR and CAT are indistinguishable; therefore $f_{RuR} = f_{CAT} = f$. Q_{PX} is the surface density of all negatively charged lipids, complexed and free. It is equal to

$$Q_{PX} = \frac{[PX]}{P_{PX}[PX] + P_{PC}[PC]}, \quad (8)$$

where the denominator is the membrane surface area per unit volume of liposome suspension.

Model B

Model B assumes no lipid-specific adsorption; both ions compete for the free, unoccupied, membrane surface. The membrane surface area balance is

$$(RuR)_m P_{sRuR} + (CAT)_m P_{sCAT} + A_f = 1. \quad (9)$$

It is convenient to consider each term as the fractional area, viz. the first term represents the area occupied by RuR, the second term that by monovalent cations, and A_f the unoccupied area available for binding. P_{sRuR} and P_{sCAT} are adsorption site areas defined as the membrane surface areas within which adsorption of other ions is excluded. The density of sites available for adsorption of RuR and CAT, needed in Langmuir equations (Eq. 3), is given by

$$f_{RuR} = A_f/P_{sRuR} \qquad f_{CAT} = A_f/P_{sCAT}. \quad (10)$$

The theoretical distribution isotherm is obtained by solving a set of equations for adsorption model A (Eqs. 1–8) or model B (Eqs. 1–6, 9, 10).

MATERIALS AND METHODS

Adsorption of RuR to liposomes was studied by using a spectrophotometric method. The measurements were based on the comparison of absorbance of two samples: one contained RuR in buffer solution (reference) and the second one (test sample) contained the solution of RuR after equilibration

with liposomes. The test sample had originally the same RuR concentration as the reference solution. Before the spectrophotometric measurements the RuR-containing liposome suspension (test sample) was processed in several freeze-and-thaw cycles (FAT cycles) to achieve an equilibrium distribution of RuR. The liposomes were subsequently pelleted in a centrifugation step, and the UV/VIS spectrum of the supernatant was compared with that of the reference RuR solution. The difference in optical absorbance, together with the data on lipid content in the suspension, was used to characterize the adsorption of RuR to lipid membranes.

Chemicals

Potassium phosphate-dibasic trihydrate ($K_2HPO_4\cdot3H_2O$) and boric acid (H_3BO_3) (Mallinckrodt Chemicals, St. Louis, MO), potassium citrate-monohydrate ($K_3C_6H_5O_7\cdot H_2O$; Matheson Coleman and Bell Manufacturing Chemists, Norwood, OH), and chloroform (American Burdick and Jackson, Muskegon, MI) were at least reagent grade. L-α-Phosphatidylcholine (egg yolk, PC, MW 760.09), L-α-phosphatidyl-serine (brain, PS, MW 810.03), L-α-phosphatidylinositol (bovine liver, PI, MW 909.12), and L-α-phosphatidylglycerol (egg-sodium salt, PG, MW 771) were bought in various concentrations from Avanti Polar Lipids (Alabaster, AL). The phospholipids were dissolved in chloroform and were all 99% pure. Ruthenium red (RuR, MW 858.5) was obtained from Fluka (Fluka Chemie AG, Buchs, Switzerland; listed purity 90–95%). All chemicals were used without further purification.

Sample preparation

Liposomes

Chloroform solutions of PC, and PS, PI, or PG were mixed in different mass ratios in 50- or 100-ml round-bottom flasks and diluted with chloroform to a final volume of no more than half the flask volume. The chloroform was slowly evaporated in a rotary flash evaporator (Buchler Instruments, Fort Lee, NJ), leaving a thin lipid film on the inside wall of the flask. The remaining chloroform was removed from the flask with a rotary pump connected to the flask for at least 1 h (more for higher lipid concentrations). In the next step a measured volume of the buffer solution was added to the flask, which was then filled with nitrogen gas. Gentle shaking removed the lipid film and produced a suspension of multilamellar liposomes with a predetermined lipid concentration. All experiments were carried out in potassium phosphate/citrate/borate (KPCB) buffer solutions with molar ratios 0.002/0.002/0.0005 M titrated to pH 7.3 with KOH. All studies were carried out at room temperature.

Ruthenium red

RuR was dissolved in buffer solution in a polycarbonate tube and heated to 60°C under continuous stirring. The solution was then centrifuged at 100,000 $\times$ g (20°C) for 2 h to remove particles and undissolved RuR. Stock solutions were prepared at least 1 day in advance and used for no more than 5 days after preparation. Solutions were kept in the refrigerator.

Actual RuR concentrations were determined spectrophotometrically by the method described by Luft (1971a). Luft reported the absorbance of purified RuR in water to be 1.583 at 533 nm (measured in 10-mm quartz cells) for a concentration of 2.34 $\times$ 10^{-5} M. Furthermore, to correct the RuR absorbance for the effect of impurities we used Luft's formula:

$$A_{RuR,\,corrected} = A_{533\,nm} - (0.20\,A_{360\,nm} + 0.25\,A_{734\,nm}), \quad (11)$$

which corrects the absorbance at the RuR peak (533 nm) for overlaps of ruthenium brown (RuB, peak at 360 nm) and ruthenium violet (RuV, peak at 734 nm).

Because we found similar absorbance values of RuR in water and in KPCB buffer, this method was used. A calibration curve confirmed that, within the range of concentrations used, there was a linear relationship

between RuR concentration and the absorbance. The above formula was not usable for centrifuged liposome suspensions because remaining lipids, due to light scattering, introduced additional absorbance at 360 nm. For these samples $A_{360\,nm}$ was replaced by $A^*_{360\,nm}$.

$$A^*_{360\,nm} = R_A A_{533\,nm}, \qquad (12)$$

where parameter $R_A = A_{360\,nm}/A_{533\,nm}$ is the ratio of absorbances at $A_{360\,nm}$ and $A_{533\,nm}$ for RuR solutions without liposomes. (We have established that the UV/VIS spectra of the supernatant can be understood as a superposition of apparent absorbance from light scattering due to residual lipids and a conventional spectrum of RuR. To avoid using experimental absorbance at 360 nm, which is strongly affected by the residual lipids, when correcting for the presence of RuB impurity, the parameter R_A provides a better method of correction.)

When the spectrophotometrically obtained RuR concentration was compared with that obtained gravimetrically, significant differences between listed and actual dye contents were found. Fluka-RuR (listed dye content 90–95%) actually contained only about 20–25% of RuR. (It may be useful for others to know that Fluka uses a chloride titration as the purity test. We found that the data provided by the company are misleading because most RuR impurities contain chloride as the counter-ion.)

Adsorption measurements

Experimental procedure

RuR stock solutions were diluted and mixed with the same volume of liposomes or buffer in polypropylene tubes. Final volumes were between 2 and 4 ml. The tubes were filled with nitrogen and vortexed briefly. Tubes containing the lipids were frozen in liquid nitrogen, thawed in water at 25°C, and vortexed for a few seconds (tubes made from glass or polystyrene tended to break during this process). It was found that five FAT cycles are sufficient to reach an equilibrium distribution of RuR. In the next step, the lipid containing solution was centrifuged at 100,000 × g (20°C) for 2 h. Pellet and supernatant were separated immediately after centrifugation. Neither the FAT procedure nor the centrifugation protocol had a measurable effect on the RuR concentration.

For spectrophotometric measurements a Beckman DU-7 spectrophotometer was used (Beckman Instruments, Irvine, CA). Either semi-micro cells made from UV grade methacrylate or self-masking micro cells made from Spectrosil were used. Each cell had a 10-mm optical path length. Because of the variations in path length, the plastic cells were calibrated by using RuR-saturated quartz cells. Plastic cells were used whenever possible because they were much less stained by RuR solutions.

Characterization of the RuR-liposome system

Ruthenium red

Fig. 1 a illustrates a typical spectrum of commercially available ruthenium red: a main peak at 535 ± 1 nm (RuR) with a slight shoulder at about 480 to 500 nm, a very broad peak at 735 ± 5 nm of ruthenium violet (RuV), a small peak at 362 ± 3 nm due to ruthenium brown (RuB), and a sharp peak at 256 ± 1 nm with a broad shoulder around 300 nm. The spectrum can be understood qualitatively using the spectra of pure RuR impurities given by Luft (1971a) as a reference. Luft reported absorption peaks of RuR at 533 nm, RuV at 734 nm, and RuB at 360 and 460 nm. A superposition of the 533 nm RuR peak and the 460 nm RuB peak accounts for the slight shoulder and the average 2-nm offset of the RuR peak observed in our batch. (RuR shows another smaller peak at 376 nm. Luft reported the absorbance ratio of these peaks $A_{533\,nm}:A_{376\,nm}$ to be 10.9 in another work (Fletcher et al., 1961); the ratio was found to be 9.8. Because we found $A_{533\,nm}:A_{376\,nm} = 5 \pm 0.6$, it is likely that half of the RuB peak is caused by RuR. The 376-nm RuR peak also causes the average 2-nm offset of the RuB peak.) The absorption peak at 256 nm is most likely caused by nitrosylruthenium impurity.
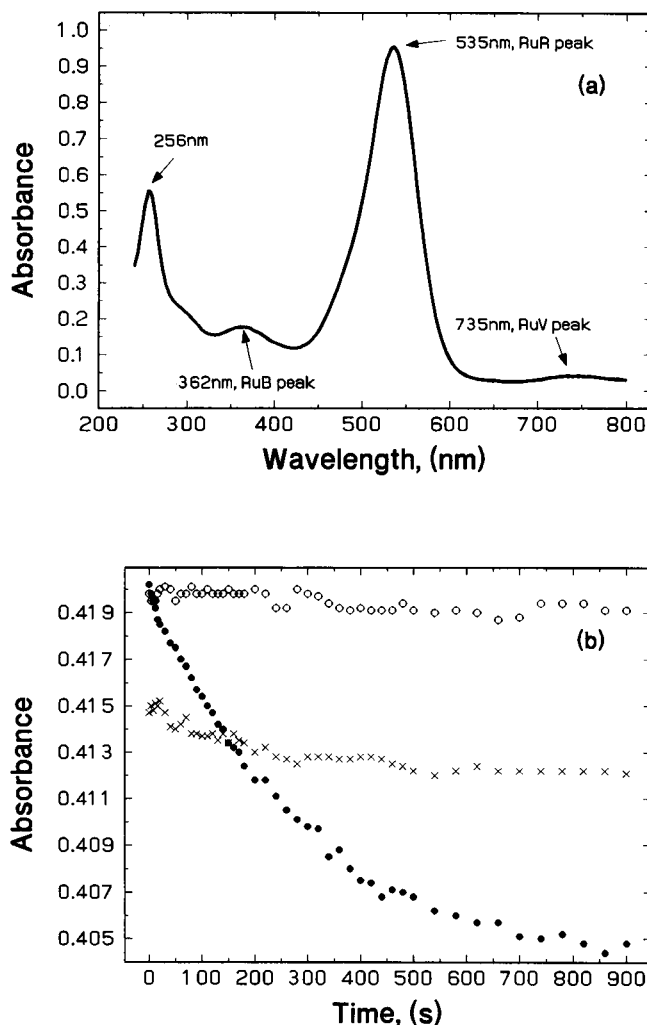

FIGURE 1 Properties of ruthenium red. (a) UV/VIS absorption spectrum in KPCB buffer (1.34 × 10^{-5}M RuR, 1 cm quartz cells). (b) Interaction of RuR with spectrophotometric cells: ●, clean quartz cells; ○, saturated quartz cells; ×, clean plastic cells. A difference in optical path length causes the absorbance offset between ○ and ×.

Luft lists three other potential impurities: ruthenium (III) hexamine trichloride (273 nm), ruthenium (III) chloropentamine dichloride (327 nm), and nitrosylruthenium (250 nm). Hochmann et al. (1981) reported 275 nm for the peak of ruthenium (III) hexamine trichloride and 323 nm for ruthenium (III) chloropentamine dichloride.

Based on spectrophotometric measurements, the purity of RuR in the batch used in our studies was 21 ± 3%.

Time stability of RuR solutions

Spectra of RuR solutions were monitored for 50 days. During this time the solutions changed their color from magenta to reddish brown to clear. We found an exponential decay of RuR absorbance (533 nm RuR peak) for both KPCB and HEPES buffer solutions at pH 7.3. Within about 30 days the absorbance values decreased to 37% of the initial readings.

Interaction of RuR with glassware

We found that RuR strongly adsorbed to all conventional laboratory glassware. We therefore replaced all glass containers and tubes with plastic

ones. No measurable adsorption to polycarbonate, polypropylene, or polystyrene was found.

Fig. 1 *b* illustrates the interaction of RuR with the two different kinds of cells. Clean quartz cells strongly adsorbed RuR, and their surface became saturated after about 15 min. When the saturated cells were filled with the same RuR solution without intermediate cleaning almost no additional adsorption of RuR was observed. Clean plastic cells showed far lower affinity to RuR than clean quartz cells. All plastic cells were calibrated for optical path length with two saturated quartz cells.

FAT cycle characterization

Two sets of experiments were done to optimize and characterize the FAT procedure. In the first set we measured the RuR concentration in the supernatant of a centrifuged RuR-liposome suspension as a function of the number of FAT cycles (Fig. 2 *a*). Adsorption of RuR to liposomes was proportional to the difference between the initial and the final, equilibrium concentration of RuR. Only weak adsorption of RuR was observed without the FAT procedure. This indicated that adsorption occurred to the outermost layers of multilamellar liposomes. RuR adsorption increased with each successive FAT cycle for up to 4 FAT cycles. For 4 or more FAT cycles RuR adsorption appeared to decrease, which was an experimental artifact caused by fragmentation of liposomes and the difficulty of pelleting small particles by centrifugation. We found, in agreement with Mayer and co-workers (Mayer et al., 1985), that 5 FAT cycles was optimal.

Changes of particle size distribution during the FAT procedure were characterized in another set of experiments. We have used Ångström's relationship (1929) between the apparent absorbance and the wavelength of light,

$$A \propto \lambda^{-\alpha}, \tag{13}$$

according to which light scattering from particles should produce a straight line in a log-log plot of the absorbance versus wavelength. The slope of this line, α, gives qualitative information about the particle size. The exponent α can change between 0, for Thomson scattering, and 4, for Rayleigh scattering. For a suspension of liposomes with a fixed amount of lipids, an increase of absorbance at a certain wavelength indicates an increase in the density of particles with a diameter comparable to that wavelength. Fig. 2 *b* shows a log-log plot of the apparent absorbance due to scattering as a function of the wavelength for a liposome suspension subjected to a different number of FAT cycles. Values of α ranged from 1.2 (no FAT) to 2.9 (9 FAT cycles); for 5 FAT cycles $\alpha = 2.6$. Data in Fig. 2 *b* illustrate that FAT procedure causes a decrease of absorbance at long wavelengths, which is compensated by its increase at short wavelengths. These spectral changes can be used to parameterize the changes of the particle size distribution in FAT processing of liposomes.

Liposome size distribution

Electron micrographs of liposomes were taken on a Hitachi HS-7S transmission electron microscope (Hitachi Instruments, San Jose, CA) at 50 kV acceleration voltage. Samples were stained by adding ruthenium red. Drops of the suspension were placed onto a carbon-coated grid and dried.

Fig. 2 *c* shows the particle size distribution in the liposome suspension after 5 FAT cycles. The total number of particles counted, which were mainly single-layered liposomes, was 268. The solid curve represents a fit of a theoretical particle size probability distribution (Winterhalter and Lasic, 1993):

$$\omega(R) \propto \frac{R}{R_m^2} \exp\left[-\left(\frac{R}{2R_m}\right)^2\right], \tag{14}$$

where ω is the probability of finding a vesicle with radius R (in nm). R_m for liposomes subjected to 5 FAT cycles was 103 nm.
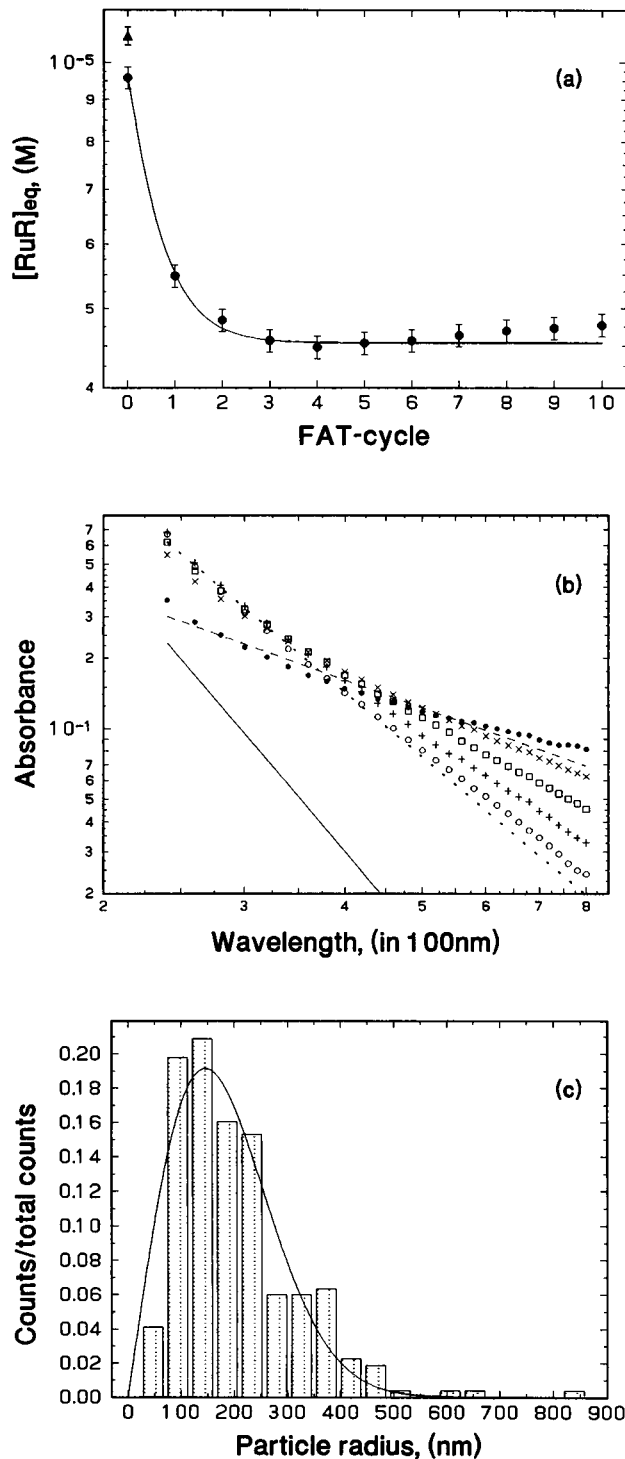

FIGURE 2   Properties of liposomes. (*a*) FAT cycle-dependent adsorption of RuR to liposomes (PC:PS 9:1 at 1 mg/ml lipid concentration, 1.03×10^{-5} M RuR, 2 h centrifugation at $100,000 \times g$). ▲, initial RuR concentration; ●, RuR concentration after FAT. The solid line represents an exponential fit to the 0 to 5 FAT cycle data. (*b*) Effect of FAT processing on the wavelength dependence of apparent absorbance due to light scattering by liposomes (PC:PS 9:1, 0.17 mg/ml lipid concentration). ●, ×, □, +, ○, data for 0, 1, 2, 5, 9 FAT cycles, respectively. The dashed and dotted lines represent fits for 0 and 9 FAT cycles. The corresponding values of α in Angström's proportionality are 1.2 and 2.9. The solid line represents the Rayleigh slope ($\alpha = 4$). (*c*) Size distribution of liposomes after 5 FAT cycles (PC:PS 9:1). The solid line represents a fit of the data to a theoretical particle size model (Eq. 14).

RESULTS

We measured adsorption of RuR to PC, PC-PS, PC-PI, and PC-PG membranes by determining the dependence of ratio R_{RuR} (Eq. 1) on the total concentration of RuR in liposome suspension. The measurements were done with FAT liposomes prepared with various proportions of zwiterionic PC and negatively charged lipids (19:1, 9:1, 4:1 at 1.0 mg/ml lipid concentration; Fig. 3) and in suspensions with various lipid concentrations (0.3, 1.0, 3.0, 10 mg/ml at a ratio 9:1 of uncharged to charged lipids; Fig. 4). RuR concentrations were calculated from the absorbance data using Luft's formula Eq. for RuR solutions and using the modified formula (Eq. 11) for the supernatant (centrifuged solutions contained residual lipids). We examined two versions of the Langmuir-Stern-Grahame adsorption model. Fits of the adsorption models A and B to experimental data were done numerically. The quality of the fits was checked visually, and the best parameters were determined by minimizing a weighted γ^2, viz.

$$\chi^2 = \frac{1}{N_{points} - N_{par}} \sum \frac{(R_{i,exp} - R_{i,th})^2}{\sqrt{(R_{i,exp} \cdot R_{i,th})}}, \quad (15)$$

where R_i is the distribution ratio for RuR concentration point i.

Effect of negatively charged lipids in PC-PS, PC-PI, and PC-PG membranes

In Fig. 3 a we present the distribution isotherms obtained for pure PC membrane (open symbols) and for PC-PS membranes with different content of PS. For pure PC membranes the distribution ratio R_{RuR} remained unity, indicating that the adsorption of RuR to PC membranes was not measurable. Adsorption of RuR was not measurable even when the lipid concentration was increased to 10 mg/ml. This finding confirms that the nonelectrostatic component of RuR binding to PC is rather weak.

Adsorption of RuR became measurable in the presence of negatively charged lipids, such as PS (Fig. 3 a), PI (Fig. 3 b), and PG (Fig. 3 c). For example, when the membrane contained about 5% PS (PC:PS ratio 19:1) the distribution ratio R_{RuR} decreased from 1.0 to ~0.5, indicating that ~50% of RuR became bound to liposomes. Adsorption of RuR to similar PI- and PG-containing membranes was less.

The lower values of distribution ratio R_{RuR} for 9:1 and 4:1 PC-PS, PC-PI, and PC-PG membranes demonstrate the enhancement effect of membrane surface charge. For the most strongly charged 4:1 PC-PS membranes ~99% of RuR originally present became bound to liposomes and ~1% remained in the aqueous phase. Binding of RuR to similar PC-PI and PC-PG was always smaller.

Qualitatively, the origin of the enhanced RuR binding with increasing surface density of negatively charged phospholipids is due to the increased RuR concentration at the aqueous side of the membrane-water interface. (At low RuR

FIGURE 3 Effect of surface charge density on adsorption of RuR to phospholipid membranes. RuR concentration dependence of the equilibrium distribution ratio for membranes with different content of negatively charged lipids (PX). Molar ratios PC:PX are 19:1 (▲), 9:1 (●), and 4:1 (◆). Lipid concentration 1 mg/ml. (a) Pure PC (○) and PC-PS. (b) PC-PI. (c) PC-PG. The curves illustrate the fit of the adsorption model for parameters given in Table 1.
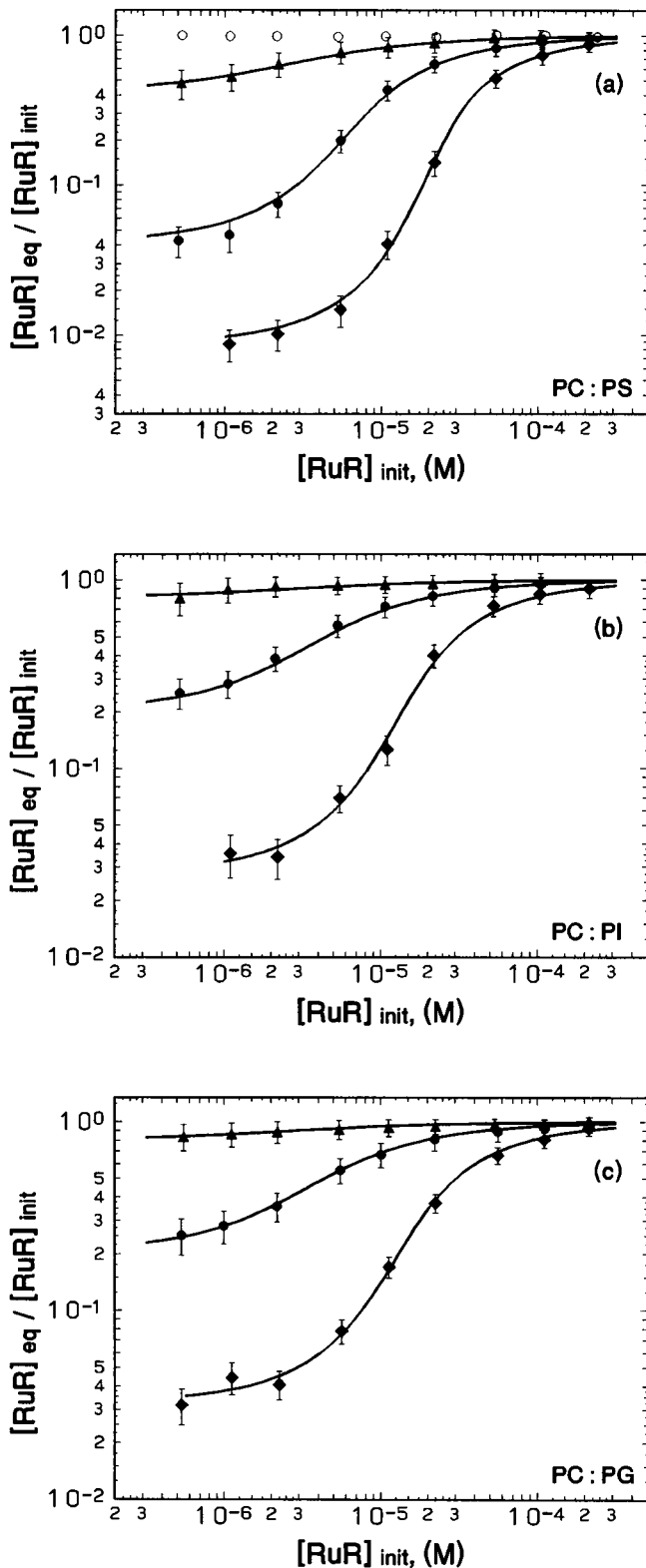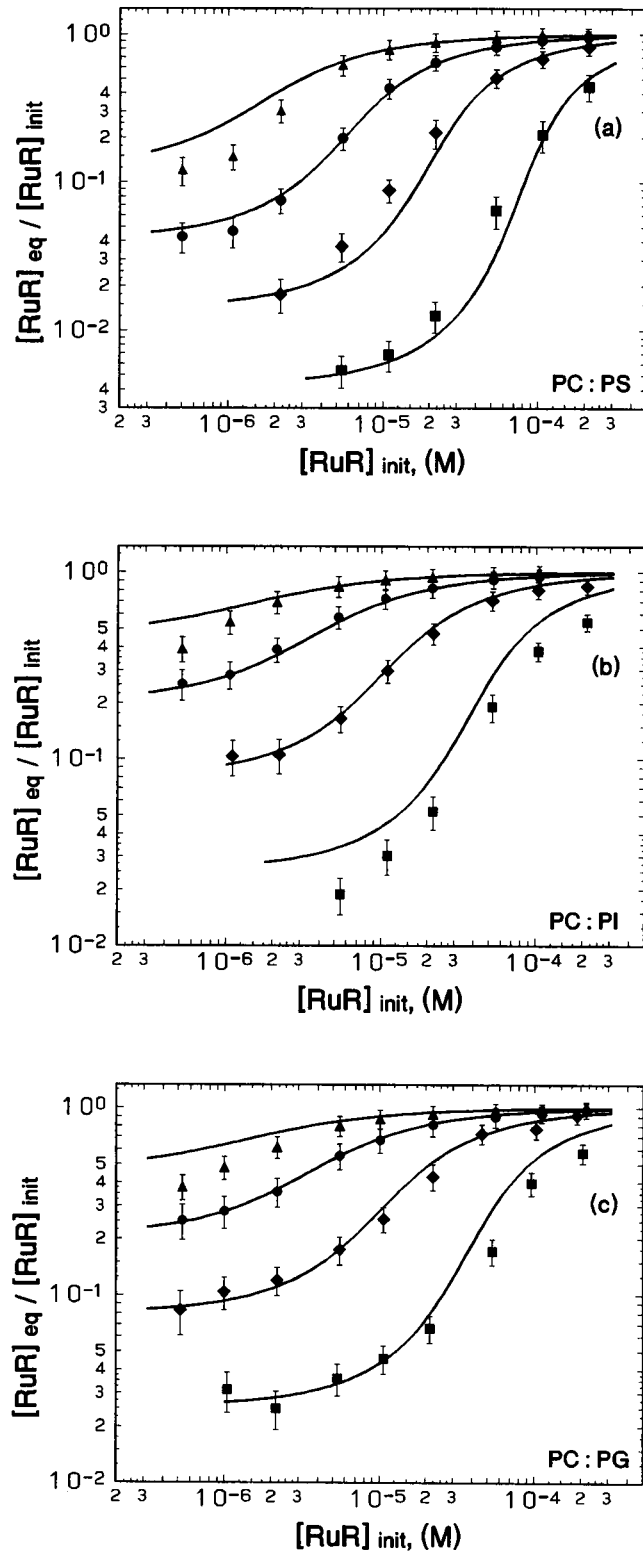
FIGURE 4 Effect of lipid concentration on adsorption of RuR to lipid membranes. RuR concentration dependence of the equilibrium distribution ratio for suspensions with different lipid content: 0.3 mg/ml (▲), 1.0 mg/ml (●), 3.0 mg/ml (◆), and 10 mg/ml (■). (a) PC-PS. (b) PC-PI. (c) PC-PG. The curves illustrate the fit of the adsorption model for parameters given in Table 1.

concentration the surface potential of liposomes is determined only by the screening effect of the buffer solution and adsorbed potassium ions. For 19:1 PC:PS, PC:PI, and PC:PG membranes we estimate the surface potential to be ~ -40 mV. The Boltzmann factor, $\exp(-6eV_m/kT)$, predicts the interfacial concentration of RuR to be $\sim 1.5 \times 10^4$ greater than the bulk RR concentration. Binding of RuR becomes measurable because the surface density of bound RuR is linearly proportional to the interfacial concentration of RuR.) This is the primary effect observed with all three types of membranes. Quantitatively, the increase of the interfacial concentration depends on the magnitude of the Boltzmann factor (Eq. 4). There were secondary, lipid-dependent variations in the degree of adsorption of RuR; the strongest binding was observed for PC-PS membranes. Affinity of RuR to PG- and PI-containing membranes was about the same but lower compared to PC-PS.

The dependence of the distribution ratio R_{RuR} on the concentration of RuR can be understood in terms of the screening and neutralization of the negative membrane surface charge. At low RuR concentrations the change in the membrane surface charge density caused by the adsorbed RuR was insignificant. Consequently, the slope of the distribution isotherm is small. As the RuR concentration increased, the negative charge on the membrane became more screened by the free RuR and partially neutralized by the adsorbed RuR. These two mechanisms decrease the membrane surface potential, which in turn reduces the magnitude of the Boltzmann factor (Eq. 4). In this regime the interfacial concentration of RuR does not proportionately increase with the bulk RuR concentration. The consequence is smaller than proportional incremental binding of RuR. As the magnitude of the membrane surface potential V_m decreases further, the distribution isotherm ultimately approaches unity at high RuR concentration.

We have found it impossible to fit the data with either variant of the adsorption model (see Theory) using the Boltzmann factor $\exp(-6eV_m/kT)$. This Boltzmann factor overestimates the interfacial concentration of RuR and thus overestimates RuR adsorption. It was found necessary to introduce an effective valency for RuR, $z_{RuR, eff}$ (Eq. 4), whose value was obtained from the fit of the model to the data (see below).

Dependence of distribution isotherms on lipid concentration

The amount of lipids in the suspension determines the membrane surface area available to adsorption, and in this way it affects the value of the distribution coefficient R_{RuR}. We have measured the distribution isotherms for different total concentrations of lipids to obtain the binding parameters of adsorption models. The experimental distribution isotherms for PC-PS, PC-PI, and PC-PG liposomes as a function of the total lipid concentration in the suspension are given in Figs. 4. The ratio of uncharged to charged lipids

was set at 9:1, and the lipid concentration was varied from 0.3 to 10 mg/ml. Two features of the experimental isotherms are noticeable. First, as the concentration of lipids increased, the distribution ratio decreased because greater membrane surface area resulted in greater degree of depletion of RuR in the aqueous phase. Second, the distribution isotherm shifted toward greater RuR concentration with increasing lipid concentration. This property is also a consequence of greater membrane surface area: greater initial concentration of RuR was needed to reduce the membrane surface potential V_m, resulting in the reduction of the Boltzmann factor. Consequently, the steep increase in the distribution ratio R_{RuR} takes place at higher RuR concentrations.

Adsorption parameters of RuR for PC-PS, PC-PI, and PC-PG membranes

To fit the Langmuir-Stern-Grahame model to experimental results it was found necessary, for both versions of the model, to introduce effective valency $z_{RuR, eff}$ of RuR ions. (Model A assumes competition between monovalent salt cations of the buffer and RR ions for the negatively charged lipids. In contrast, in model B the adsorption of both types of ions is nonspecific to the type of lipids; ions compete only for the free available surface.) A lower value of effective valency accounts for nonideal behavior of RuR within the diffuse double layer.

The solid curves in Figs. 3 and 4 illustrate the distribution ratio of RuR predicted from adsorption model A. Two model parameters were optimized: the effective valency of RuR ions, $z_{RuR, eff}$, and the association constant of RuR for negatively charged lipids, K_{mRuR}. Adsorption of potassium ions to negatively charged lipids was accounted for by association constant $K_{mCAT} = 1.0$ M^{-1}, as in other ion adsorption studies (Langner et al.,1990). The adsorption parameters for all three types of membranes obtained from the best fit of model A are given in Table 1. There are several notable characteristics in the results. First, the PC-PS, PC-PI, and PC-PG membranes are electrostatically equivalent. A single value of effective valency of RuR ions was found for the same fixed ratios of uncharged and charged lipids in all three types of membranes. Second, the

dependence of distribution isotherms on the concentration of lipids can be fitted with a single value for the association constant, one for each type of lipid: $K_{mRuR} = 5.5$ M^{-1} for PS and $K_{mRuR} = 0.9$ M^{-1} for both PI and PG. Third, the adsorption data indicate that RuR ions do not behave as hexavalent species within the Gouy-Chapman diffuse double layer. For the weakly charged (19:1) membranes the effective valency was found to be 5.0 ± 0.3. It decreased with increasing density of the negative surface charge to 3.1 $\pm$ 0.1 for the strongly charged membranes (4:1).

The experimental results shown in Figs. 3 and 4 can be equally well fit with model B, which does not assume specific adsorption of ions to negatively charged lipids (theoretical curves not shown). This model does not exclude possible adsorption of RuR to PC. (It is conceivable that adsorption of RR to PC also takes place, but it is significant only because of the concentrating effect of negatively charged membrane surface, as reflected by the Boltzmann factor.) It is of interest to compare the adsorption parameters obtained from the fit of models B and A. Again, it was found impossible to fit the data by means of association constants and adsorption site areas, even when all possible systematic experimental errors were considered. It became necessary to invoke effective valency $z_{RuR, eff}$ as in model A. To keep the number and the type of parameters in model B the same as in model A, i.e., $z_{RuR, eff}$ and K_{mRuR}, we have set the adsorption site areas for RuR ions to $P_{sRuR} = 5.0$ nm^2 and that for potassium ions to $P_{sCAT} = 0.72$ nm^2. P_{sRuR} was estimated as the ion exclusion area using a simple electrostatic argument (Smejtek and Wang, 1990), and P_{sCAT} was made equal to the membrane surface area of hydrated egg PC (Small, 1986).

Table 2 summarizes the best values of $z_{RuR, eff}$ and K_{mRuR} obtained from the fit of model B to data shown in Figs. 3 and 4. Because it was uncertain how to treat adsorption of potassium ions to the mixed lipid membranes, the analysis was done for two cases. In case i) adsorption of potassium was ignored ($K_{mCAT} = 0$), and in case ii) adsorption of potassium was slightly overestimated ($K_{mCAT} = 1.0$ M^{-1}). $z_{RuR, eff}$ and K_{mRuR} given in the left column in Table 2 correspond to an assumed absence of adsorption of potassium (case i); those in the right column correspond to conditions in which potassium ion adsorption was overestimated (case ii). It is noteworthy that the patterns in the values of the adsorption parameters for model B and model A are similar. The effective valency of RuR ion decreased with the increasing presence of negatively charged lipids in the membrane, and the ratios of association constants for PC-PS and PC-PI or PC-PG membranes were about the same as in model A. Furthermore, the values of binding parameters obtained from model B overlap with those obtained for model A.

Fig. 5 illustrates how the effective valency of RuR ion, obtained from the fit of model A, depends on the density of electric charge on the membrane's surface. The effect of reduced valency of RuR follows from the overestimation of the concentration of RuR ions at the membrane/water inter-

TABLE 1 Adsorption parameters, model A

	19:1	9:1	4:1
PC:PS			
$z_{RuR, eff}$	5.0 ± 0.3	3.9 ± 0.2	3.1 ± 0.1
K_{mRuR} (M^{-1})	5.5 ± 2.5	5.5 ± 2.0	5.5 ± 1.5
PC:PI			
$z_{RuR, eff}$	5.0 ± 0.3	3.9 ± 0.2	3.3 ± 0.1
K_{mRuR} (M^{-1})	0.9 ± 0.4	0.9 ± 0.3	0.9 ± 0.2
PC:PG			
$z_{RuR, eff}$	5.0 ± 0.3	3.9 ± 0.2	3.3 ± 0.1
K_{mRuR} (M^{-1})	0.9 ± 0.4	0.9 ± 0.3	0.9 ± 0.2

TABLE 2   Adsorption parameters, model B

	19:1		9:1		4:1	
PC:PS						
$z_{RuR, eff}$	4.3 ± 0.3	6.9 ± 0.5	3.6 ± 0.2	5.5 ± 0.3	2.9 ± 0.1	4.3 ± 0.2
K_{mRuR} (M^{-1})	3.2 ± 1.5	8.0 ± 3.0	3.2 ± 1.0	8.0 ± 2.5	3.2 ± 0.8	8.0 ± 2.0
PC:PI						
$z_{RuR, eff}$	4.3 ± 0.3	6.9 ± 0.5	3.6 ± 0.2	5.5 ± 0.3	3.0 ± 0.1	4.5 ± 0.2
K_{mRuR} (M^{-1})	0.6 ± 0.25	1.3 ± 0.4	0.6 ± 0.2	1.3 ± 0.3	0.6 ± 0.15	1.3 ± 0.2
PC:PG						
$z_{RuR, eff}$	4.3 ± 0.3	6.9 ± 0.5	3.6 ± 0.2	5.5 ± 0.3	3.0 ± 0.1	4.5 ± 0.2
K_{mRuR} (M^{-1})	0.6 ± 0.25	1.3 ± 0.4	0.6 ± 0.2	1.3 ± 0.3	0.6 ± 0.15	1.3 ± 0.2

Values on the left side of each column correspond to $K_m(CAT) = 0.0$; those on the right side were obtained for $K_m(CAT) = 1.0$ M^{-1}.

face. As the data indicate, the magnitude of this discrepancy increases with the increasing density of membrane surface charge.

DISCUSSION

This work has shown that the presence of negatively charged phospholipids in lipid bilayer is essential for the adsorption of RuR cations to phospholipid membrane, although it is not clear whether the adsorption is lipid specific or not, because models A and B provided very similar adsorption parameters. Another feature of the results is that it became necessary to invoke an effective charge of the RuR cation, which turned out to be smaller than the physical charge of $+6e$. We have examined the potential impact of impurities in the commercial samples of RuR and concluded that the impurities cannot meaningfully alter the above results. (It is important to keep in mind that commercially available RuR used in this study as well as in others reported in the literature was not pure and that some of the impurities present in RuR are ionic. The two possible processes in which the ionic impurities would affect our results are i) reduction of membrane surface potential below the

FIGURE 5   Dependence of effective valency of the RuR cation on surface charge density of PC-PS, PC-PI, and PC-PG membranes obtained from the fit of model A.

value expected from the content of negatively charged lipids in the membrane due to additional screening and ii) adsorption to the membrane. Therefore, association constants given in this paper should be considered as the lower limit for pure RuR. However, we have several reasons to believe that our values are only slightly affected by impurities: a) The adsorption parameters for RuR are primarily determined by the values of the distribution ratio within the low RuR concentration segment. Within this range the ionic screening is determined by the KPCB buffer and not by RuR, and therefore not by impurities in RuR. b) The predictions of the adsorption model indicate only low surface coverage by RuR in the low RuR concentration range; this means that competition of RuR for unoccupied negatively charged lipids (model A) or free membrane surface (model B) would not limit RuR adsorption. c) We did not observe changes in the UV/VIS spectrum that were not caused by RuR. Furthermore, we have verified the stability of our results and conclusions against the effect of impurities using our computer model by assuming the presence of 45% ruthenium brown (with adsorption properties similar to RuR) in addition to RuR.)

The "anomalous" behavior of charged molecules at membrane-water interfaces is often discussed in terms of the discreteness of charge. The membrane charges due to negatively charged lipids dispersed in the matrix of electrically neutral lipids are discrete, whereas the Gouy-Chapman model of the diffuse double layer assumes membrane charge smeared at the membrane surface (Nelson and Mc-Quarrie, 1975; Andersen et al., 1978; Wang and Bruner, 1978; Schoch and Sargent, 1980; Tsien and Hladky, 1982; Schwartz and Beschiaschvili, 1989; Beschiaschvili and Seelig, 1990). Probing the concentration of co-ions and counter-ions in the vicinity of the charged membrane surface by fluorescence, EPR probes and ζ-potential methods indicated that the Langmuir-Stern-Grahame model described remarkably well the experimental results when membranes contained singly charged lipids (Winiski et al., 1986; Langner et al., 1990), as in our case. Anomalies were found for PC membranes containing negatively charged trivalent lipids, phosphatidylinositol 4,5-biphosphate, PIP_2 (Langner et al., 1990). What is most interesting is that
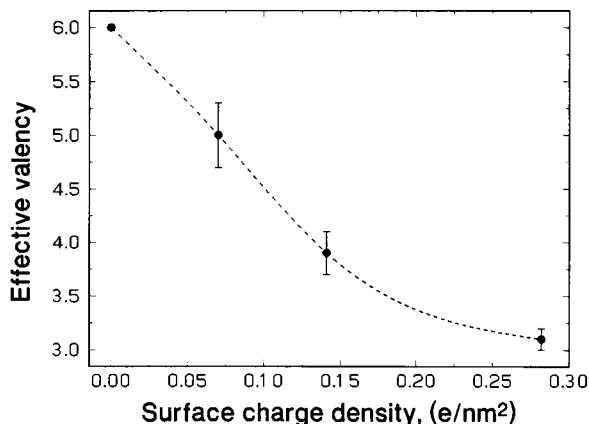
anomalies were found for the distribution of negatively charged probes, i.e., of co-ions, whereas dominating effects due to the discreteness of charge were expected for the counter-ions (Nelson and McQuarrie, 1975). In general, the Gouy-Chapman-Stern theory was found to be satisfactory for the description of membrane surface potential and ion adsorption for monovalent as well as multivalent counterions along with PC membranes containing monovalent, acidic lipids (McLaughlin and Harary, 1976; Lau et al., 1981; McLaughlin et al., 1981; Chung et al., 1985; McLaughlin, 1989; Graham et al., 1990; Smejtek and Wang, 1990; Tatulian, 1993, 1994), as well as for Ca^{2+} adsorption and dependence of Ca^{2+} adsorption on ionic strength for ATPase in SR membranes (Scofano et al., 1985).

Is the anomalous behavior of RuR due to the discreteness of membrane charge? In the present study the membranes contained singly charged lipids, and the adsorbing species were hexavalent counter-ions. The discrete charge effects are generally expected to be prominent when the separation between charges is greater than the Debye length. In our system the average separation between negative phospholipids varied from 3.8 nm (19:1 membranes) to 1.9 nm (4:1 membranes), and the Debye length of the aqueous medium remained $\sim$2.5 nm, within the greater portion of the experimental RuR concentration range. Because the separation between charges and the Debye length was comparable and considering the computed electrostatic potential distribution for charged membranes using a nonlinearized Poisson-Boltzmann equation (Peitzsch et al., 1995), the discrete charge effects are not expected to be prominent in the present work. Furthermore, estimates of the Boltzmann factor based on a simple discrete charge model (Nelson and McQuarrie, 1975) suggest that $z_{RuR, eff}e$ should be much greater than the physical charge of RuR, which is in conflict with our experimental finding.

Effective charges smaller than the physical charge, ze, were also reported in studies of adsorption of bee venom peptide melittin ($z_{eff} \approx 2$, in contrast to $z = 5-6$) (Schoch and Sargent, 1980; Schwartz and Beschiaschvili, 1989; Beschiaschvili and Seelig, 1990); for positively charged peptides lysine$_n$ and arginine$_n$, $z_{pentalysine, eff} \approx 2$ instead of $z = 5$ (Kim et al., 1991); for mixed peptides $z_{eff} \approx 2.5$ in contrast to $z = 5$ (Mosior and McLaughlin, 1992); and for peptides corresponding to the pseudosubstrate region of protein kinase C, $z_{eff} \approx 2.5-3$ instead of $z = 5$ (Mosior and McLaughlin, 1991). It was assumed that the effect of reduced charge of these large peptides was associated with the discreteness of membrane charge, partial neutralization, and finite size of the peptides. It is interesting that Stankowski's model (1991) predicts $z_{eff} < z$, as observed in the binding studies with peptides. It is not clear a priori that the origin of "anomalous" behavior of peptides and RuR is the same.

Another possible origin of reduced effective charge of multivalent ions is the formation of complexes. It is conceivable that RuR^{6+} would form complexes with counterions, such as OH^-. However, if such mechanisms were

effective in the adsorption of RuR, the concentration of $RuR^{6+} \cdots nOH^-$ complexes at the membrane/water interface would decrease with the increasingly negative membrane surface potential because of the repulsion of OH^- from the membrane/water interface. According to this scenario z_{eff} is expected to increase with the increasing content of negatively charged lipids in the membrane, whereas the opposite is taking place (Fig. 5). (This argument, which eliminates the formation of $RuR^{6+} \cdots nOH^-$ complex as the origin of reduced effective charge of RuR, was contributed by the reviewer. Furthermore, RuR is stable within a narrow range of pH, which precludes studies of the effect of pH on z_{eff}.)

Reduced screening of the membrane surface by multiply charged ions and therefore reduced interfacial concentration (compared to that predicted from simple Gouy-Chapman theory) was observed for charged molecules with widely separated charges, such as hexamethonium (Carnie and McLaughlin, 1983; Alvarez et al., 1983). This effect is prominent when the Debye length is shorter than the separation between charges. RuR can be regarded as a charged cylinder of length 1.2 nm (Carrondo et al., 1980) or as a linear array of three charges separated by 0.6 nm. Under our experimental conditions the length of the RuR ion is smaller than the Debye length ($\sim$2.5 nm), and thus it is not known how effective this mechanism of reduction of the interfacial concentration of RuR would be in our case. We speculate that the effect of reduced effective charge of RuR is the consequence of the finite size of RuR and the assumption of ions as pointlike particles in the Gouy-Chapman model of the diffuse double layer. (Finite size effects are expected to be prominent for hexavalent RuR because the Boltzmann factor for pointlike RuR ions is equal to the sixth power of the Boltzmann factor for monovalent cations. This approach leads to extremely short inter-ion distances and unrealistically high concentrations of RuR within the double layer close to the membrane surface.)

It is also possible that some RuR trapped in the diffuse double layer is removed from the aqueous phase when centrifuging the liposomes. If the entrapment effect dominated the removal of RuR in our studies, we would not be able to observe differences between PC-PS, PC-PI, and PC-PG membranes. Computer modeling of this effect indicated that the S shape of the distribution isotherm, as seen in our experimental results, is possible only when adsorption of RuR takes place in addition to entrapment within the diffuse double layer. The consequence of introduction of the entrapment effect (for which we do not have data) would be an increase of the magnitude of the association constant and a decrease of effective valency. Thus the values of association constants reported here should be regarded as their lower limit and those for the effective valency as their upper limit.

It is highly desirable to measure in future studies of interaction of RuR with charged membranes the electrophoretic mobility of liposomes to determine the membrane surface potential directly and, if possible, the interfacial concentration of RuR. These quantities would provide in-

formation on the magnitude of the Boltzmann factor. New studies will require novel approaches, e.g., microelectro-phoresis with ultrasonic rather than optical detection of liposome velocity because RuR solutions are strongly colored, and use of special plastics because of strong staining of glass surfaces by RuR.

Relevance to biomembranes

Results of binding studies with phospholipid bilayers make it possible to examine the significance of the binding of RuR to the lipid bilayer matrix in biological membranes.

We consider the membrane of the sarcoplasmic reticulum (SR) as a prototype biomembrane. Although functionally complex, its composition is simple; the SR consists primarily of calcium pumps that constitute about 90% of the membrane proteins, and its lipid matrix contains a significant amount of phospholipids. In the discussion of RuR binding to SR, we assume the same molar ratio of phospholipids to protein as used in the analysis of x-ray diffraction data (Herbette et al., 1985), viz. 128 mol phospholipids/mol calcium pumps.

Based on x-ray diffraction results (Herbette et al., 1985) the Ca pumps form a lattice with unit cell size $\sim$11–12.5 nm. The outer disk of the pump covers approximately 20–40 nm^2 of membrane surface area, and the arrangement of Ca pumps corresponds to one pump per $\sim$140 nm^2 of membrane surface. Consequently, the area of the "protein-free" bilayer represents $\sim$80% of the total membrane surface of SR. These data make it possible to relate adsorption of RuR measured for phospholipid bilayers to that observed for SR membranes.

The surface charge of the SR membrane is negative, and the charge density reported in the literature is (5.4 − 9.2) × $10^{-3}C/m^2$ (Arrio et al., 1984; Liu and Oba, 1990), which corresponds to $-(0.034-0.058)e/nm^2$. The values for the surface charge density of SR were determined from the electrophoretic mobility of SR vesicles and should be regarded as the lower limiting value of surface charge density. (The reason for this caution is that the Ca pumps protrude from the SR membrane surface, so that the position of shear plane at which ζ-potential is determined is unknown. The presence of protrusions results in additional frictional force, which also have not been accounted for. The surface charge density of SR may be therefore underestimated.) We expect that the charge density of the SR membrane is comparable to that of liposomes made from mixtures of uncharged to charged phospholipids within the 19:1–9:1 range.

The density of RuR binding sites in SR membrane obtained in various studies is about 10 nmol/mg protein. Specifically, Corbalan-Garcia et al. (1992) reported RuR binding of 6 nmol/mg protein for the rabbit skeletal SR vesicles. Moutin et al. (1992) found two populations of RuR-binding sites for rabbit skeletal SR vesicles. One group of sites was found to bind $\sim$10 nmol/mg protein and was assigned to the high-affinity Ca^{2+} transport sites of the Ca^{2+}-ATPase; the other group of sites bind 15–17 nmol RuR/mg protein. This second group was thought to represent "nonspecific cation binding

sites of the SR Ca^{2+}-ATPase or of a closely associated element" (Moutin et al., 1992).

We examine now the possibility of RuR binding to the lipid matrix of SR, using our results for 19:1 and 9:1 PC:PS membranes. The RuR binding assays of biomembranes employ, typically, micromolar concentrations of RuR. Consider, for example, an equilibrium aqueous concentration $[RuR]_{eq} \approx 8 \ \mu M$. For this concentration of RuR we obtained the surface density of bound RuR as $\sim$3 $nmol/m^2$ for 19:1 PC:PS and $\sim$15 $nmol/m^2$ for 9:1 PC:PS membranes. Because the free lipid bilayer surface in the SR membrane was estimated to be 80% of the total surface, the respective surface densities of RuR in the Ca pump-containing phospholipid membrane model are $\sim$2.4 $nmol/m^2$ (for 19:1 PC:PS) and $\sim$12 $nmol/m^2$ (for 9:1 PC:PS bilayer). Furthermore, we assume that in this phospholipid matrix there is one Ca pump per $\sim$140 nm^2 of membrane surface area, as estimated from the x-ray diffraction data. Thus, for this phospholipid analog of the SR membrane, the corresponding protein mass per unit area of membrane surface is equal to $(119 \times 10^3$ g pump protein/mol)/($N_{Av} \cdot 140 \times 10^{-18}m^2) = 1.4$ mg protein/m^2. This conversion factor makes it possible to relate RuR adsorption to phospholipid bilayers to RuR adsorption in SR because adsorption to biomembranes is conventionally referenced to the amount of protein in mg. The above estimation yields a binding of 1.7 nmol RuR/mg protein for an SR analog based on 19:1 PC:PS and 8.6 nmol RuR/mg protein for 9:1 PC:PS analog. Thus, the levels of RuR binding in the model calcium pump-containing phospholipid bilayer are comparable to those obtained with native SR vesicles. These estimates illustrate that the binding of RuR to the lipid matrix may indeed represent a significant fraction of the total RuR binding in negatively charged biomembranes and support the hypothesis (Moutin et al., 1992) that the so-called low-affinity sites on SR membranes can be indeed associated with the lipid matrix.

Another relevant point to the studies of RuR adsorption on biomembranes is that in spite of small values for the intrinsic association constant of RuR with the phospholipid membranes, the adsorption of RuR to negatively charged phospholipid bilayers is significant, even at low RuR concentrations. This is due to the strong attractive force acting on hexavalent RuR ions within the diffuse double layer. The electrostatic interactions between RuR and the negatively charged membrane result in interfacial concentrations of RuR ions many orders of magnitude higher than in the bulk solution. This increased interfacial concentration of RuR shifts the binding equilibrium toward a greater density of membrane-bound RuR. Thus, regardless of the origin of binding sites, be it active sites on membrane-bound proteins or the lipid matrix, the fraction of these sites occupied by RuR is equal to

$$\theta \approx \frac{K_{mRuR}[RuR]_{eq}\exp(-z_{RuR,eff}eV_m/k_BT)}{1 + K_{mRuR}[RuR]_{eq}\exp(-z_{RuR,eff}eV_m/k_BT)}. \quad (16)$$

From this follows that 1) the product $K_{mRuR}[RuR]_{eq}$ $\exp(-\nu_{RuR,\ eff}eV_m/kT)$ determines the degree of occupancy of adsorption sites, θ, and 2) the intrinsic association constant is not the quantity obtained in conventional binding studies because the value of the Boltzmann factor, $\exp(-z_{RuR,\ eff}eV_m/kT)$, is usually unknown.

REFERENCES

Alvarez, O., M. Brodwick, R. Latorre, A. McLaughlin, S. McLaughlin, and G. Szabo. 1983. Large divalent cations and electrostatic potentials adjacent to membranes. *Biophys. J.* 44:333–342.

Amann, R., and C. A. Maggi. 1991. Ruthenium red as a capsaicin antagonist. *Life Sci.* 49:849–856.

Andersen, O., S. Feldberg, H. Nakadomari, S. Levy, and S. McLaughlin. 1978. Electrostatic interactions among hydrophobic ions in lipid bilayer membranes. *Biophys. J.* 21:35–70.

Ångström, A. 1929. On the atmospheric transmission of sun radiation and on dust in the air. *Geograf. Ann.* 11:155–166.

Arrio, B., G. Johannin, A. Carrette, J. Chevallier, and D. Brethes. 1984. Electrokinetic and hydrodynamic properties of sarcoplasmic reticulum vesicles: a study by laser Doppler electrophoresis and quasi-elastic light scattering. *Arch. Biochem. Biophys.* 228:220–229.

Beschiaschvili, G., and J. Seelig. 1990. Melittin binding to mixed phosphatidylglycerol/phosphatidylcholine membranes. *Biochemistry.* 29:52–58.

Carnie, S., and S. McLaughlin. 1983. Large divalent cations and electrostatic potentials adjacent to membranes. A theoretical calculation. *Biophys. J.* 44:325–332.

Carrondo, M., W. P. Griffith, J. P. Hall, and A. C. Skapski. 1980. X-ray structure of $[Ru_3O_2(NH_3)_{14}]^{6+}$, cation of the cytological reagent ruthenium red. *Biochim. Biophys. Acta.* 627:332–334.

Charuk, J. H. M., C. A. Pirraglia, and R. A. F. Reithmeier. 1990. Interaction of ruthenium red with Ca^{2+}-binding proteins. *Anal. Biochem.* 188: 123–131.

Chung, L., G. Kalyanides, R. McDaniel, A. McLaughlin, and S. McLaughlin. 1985. Interaction of gentamicin and spermine with bilayer membranes containing negatively charged phospholipids. *Biochemistry.* 24: 442–453.

Corbalan-Garcia, S., J. Teruel, and J. Gomez-Fernandez. 1992. Characterization of ruthenium red-binding sites of the Ca^{2+}-ATPase from sarcoplasmic reticulum and their interaction with Ca^{2+}-binding sites. *Biochem. J.* 287:767–774.

Dierichs, R. 1979. Ruthenium red as a stain for electron microscopy. Some new aspects of its application and mode of action. *Histochemistry.* 64:171–187.

Fletcher, J. M., B. F. Greenfield, C. J. Hardy, D. Scargil, and J. L. Woodhead. 1961. Ruthenium red. *J. Chem. Soc.* 2000–2006.

Graham, I., H. Barrabin, G. Inesi, and J. A. Cohen. 1990. Ion binding to charged lipid monolayers: the role of double layer and ion binding models. *J. Colloid Interface Sci.* 135:335–352.

Herbette, L., P. DeFoor, S. Fleischer, D. Pascolini, A. Scarpa, and J. K. Blasie. 1985. The separate profile structures of the functional calcium pump protein and the phospholipid bilayer within isolated sarcoplasmic reticulum membranes determined by x-ray and neutron diffraction. *Biochim. Biophys. Acta.* 817:103–122.

Hochman, J. H., B. Partridge, and S. Ferguson-Miller. 1981. An effective electron donor to cytochrome oxidase. Purification, identification, and kinetic characterization of a contaminant of ruthenium red, hexaamineruthenium II/III. *J. Biol. Chem.* 256:8693–8698.

Joly, A. 1892. Composés ammoniacaux dérivés du sesquichlorue de ruthénium. *C. R. Acad. Sci.* 115:1299–1301.

Kim, J., M. Mosior, L. A. Chung, H. Wu, and S. McLaughlin. 1991. Binding of peptides with basic residues to membranes containing acidic phospholipids. *Biophys. J.* 60:135–148.

Langner, M., D. Cafiso, S. Marcelja, and S. McLaughlin. 1990. Electrostatics of phosphoinositide bilayer membranes. Theoretical and experimental results. *Biophys. J.* 57:335–349.

Lau, A., A. McLaughlin, and S. McLaughlin. 1981. The adsorption of divalent cations to phosphatidylglycerol bilayer membranes. *Biochim. Biophys. Acta.* 645:279–292.

Liu, G., and T. Oba. 1990. Effects of tetraphenylboron-induced increase in inner surface charge on Ca^{2+} release from sarcoplasmic reticulum. *Jpn. J. Physiol.* 40:723–736.

Luft, J. H. 1971a. Ruthenium red and violet I. Chemistry, purification, methods of use for electron microscopy and mechanism of action. *Anat. Rec.* 171:347–368.

Luft, J. H. 1971b. Ruthenium red and violet II. Fine structural localization in animal tissues. *Anat. Rec.* 171:369–416.

Luthra, R., and M. S. Olson. 1977. The inhibition of calcium uptake and release by rat liver mitrochondria by ruthenium red. *FEBS Lett.* 81: 142–146.

Mangin, L. 1893. Sur l'emploi du rouge de ruthénium en anatomie végétale. *C. R. Acad. Sci.* 116:653–656.

Mayer, L. D., M. J. Hope, P. R. Cullis, and A. S. Lanoff. 1985. Solute distributions and trapping efficiencies observed in freeze-thawed multilamellar vesicles. *Biochim. Biophys. Acta.* 817:193–196.

McLaughlin, S. 1989. The electrostatic properties of membranes. *Annu. Rev. Biophys. Biophys. Chem.* 18:113–136.

McLaughlin, S., and H. Harary. 1976. The hydrophobic adsorption of charged molecules to bilayer membranes: a test of the applicability of the Stern equation. *Biochemistry.* 15:1941–1948.

McLaughlin, S., N. Mulrine, T. Gresalfi, G. Vaio, and A. McLaughlin. 1981. Adsorption of divalent cations to bilayer membranes containing phosphatidylserine. *J. Gen. Physiol.* 77:445–473.

Missiaen, L., H. De Smedt, G. Droogmans, F. Wuytack, L. Raeymaekers, and R. Casteels. 1990. Ruthenium red and compound 48/80 inhibit the smooth-muscle plasma-membrane Ca^{2+} pump via interaction with associated polyphosphoinositedes. *Biochim. Biophys. Acta.* 1023: 449–454.

Moore, C. L. 1971. Specific inhibition of mitochondrial Ca^{2+} transport by ruthenium red. *Biochem. Biophys. Res. Commun.* 42:298–305.

Mosior, M., and S. McLaughlin. 1991. Peptides that mimic the pseudosubstrate region of protein kinase C bind to acidic lipids in membranes. *Biophys. J.* 60:149–159.

Mosior, M., and S. McLaughlin. 1992. Binding of basic peptides to acidic lipids in membranes: effects of inserting alanine(s) between basic residues. *Biochemistry.* 31:1767–1773.

Moutin, M., C. Rapin, and Y. Dupont. 1992. Ruthenium red affects the intrinsic fluorescence of the calcium-ATPase of skeletal sarcoplasmic reticulum. *Biochim. Biophys. Acta.* 1100:321–328.

Murano, E., S. Paoletti, A. Cesaro, and R. Rizzo. 1990. Ruthenium red complexation with ionic polysaccharides in dilute aqueous solutions: chirooptical evidence of stereospecific interaction. *Anal. Biochem.* 187: 120–123.

Nelson, A. P., and D. A. McQuarrie. 1975. The effect of discrete charges on the electrical properties of a membrane. I. *J. Theor. Biol.* 55:13–27.

Peitzsch, R. M., M. Eisenberg, K. A. Sharp, and S. McLaughlin. 1995. Calculations of the electrostatic potential adjacent to model phospholipid bilayers. *Biophys. J.* 68:729–738.

Reimann, B. 1961. Zur Verwendbarkeit von Rutheniumrot als elektronenmikroskopisches Kontrastierungsmittel. *Mikroskopie.* 16:224–226.

Salama, G., and J. Abramson. 1984. Silver ions trigger Ca^{2+} release by acting at the apparent physiological release site in sarcoplasmic reticulum. *J. Biol. Chem.* 259:13363–13369.

Sasaki, T., M. Naka, F. Nakamura, and T. Tanaka. 1992. Ruthenium red inhibits the binding of Ca to calmodulin required for enzyme activation. *J. Biol. Chem.* 267:21518–21523.

Schoch, P., and D. F. Sargent. 1980. Quantitative analysis of the binding of melittin to planar lipid bilayers allowing for the discrete charge effect. *Biochim. Biophys. Acta.* 602:234–247.

Schwarz, G., and G. Beschiaschvili. 1989. Thermodynamic and kinetic studies of the association of melittin with a phospholipid bilayer. *Biochim. Biophys. Acta.* 979:82–90.

Scofano, H., H. Barrabin, G. Inesi, and J. A. Cohen. 1985. Stoichiometric and electrostatic characterization of calcium binding to native and lipid-substituted adenosinetriphosphatase of sarcoplasmic reticulum. *Biochim. Biophys. Acta.* 819:93–104.

Small, D. 1986. Handbook of Lipid Research, Vol. 4. The Physical Chemistry of Lipids. Plenum Press, New York.

Smejtek, P., and S. Wang. 1990. Adsorption of dipalmitoylphosphatidyl-choline membranes in gel and fluid state: pentachlorophenolate, dipic-rylamine, and tetraphenylborate. *Biophys. J.* 58:1285–1294.

Stankowski, S. 1991. Surface charging by large multivalent molecules. Extending the standard Gouy-Chapman treatment. *Biophys. J.* 60: 341–351.

Taipale, H. T., R. A. Kauppinen, and H. Komulainen. 1989. Ruthenium red inhibits the voltage-dependent increase in cytosolic free calcium in cortical synaptosomes from guinea pig. *Biochem. Pharmacol.* 38: 1109–1113.

Tatulian, S. A. 1993. Ionization and ion binding. *In* Phospholipids Handbook. G. Cevc, editor. Marcell Dekker, New York. 511–552.

Tatulian, S. A. 1994. Evaluation of ion binding of zwitterionic membranes based on extended Gouy-Chapman-Stern theory. *J. Phys. Chem.* 98: 4963–4965.

Tsien, R. Y., and S. B. Hladky. 1982. Ion repulsion within membranes. *Biophys. J.* 39:49–56.

Vasington, F. D., P. Gazzotti, R. Tiozzo, and E. Carafoli. 1972. The effect of ruthenium red on Ca^{2+} transport and respiration in rat liver mitochondria. *Biochim. Biophys. Acta.* 256:43–54.

Wang, C., and L. Bruner. 1978. Evidence for a discrete charge effect within lipid bilayer membranes. *Biophys. J.* 24:749–764.

Watson, E. L., F. F. Vincenzi, and P. W. Davis. 1971. Ca^{2+}-activated membrane ATPase: selective inhibition by ruthenium red. *Biochim. Biophys. Acta.* 249:606–610.

Winiski, A. P., A. C. McLaughlin, R. V. McDaniel, M. Eisenberg, and S. McLaughlin. 1986. An experimental test of discreteness-of-charge effect in positive and negative lipid bilayers. *Biochemistry.* 25: 8206–8214.

Winterhalter, M., and D. D. Lasic. 1993. Liposome stability and formation: experimental parameters and theories on the size distribution. *Chem. Phys. Lipids.* 64:35–43.EQ 1 EQ 7